Structural Effects of Metallicity on Circumstellar Discs

AD2097

Department of Physics and Astronomy, University of Bath, Bath BA2 7AY, UK
e-mail: ad2097@bath.ac.uk

Received: 09 January 2023

ABSTRACT

Context. The model for circumstellar discs around Herbig AE stars considers the influence of the direct stellar radiation on the inner rim of the disc, which becomes puffed up and casts a shadow.
Aims. The study aims to understand the relationship between metallicity and the shape of circumstellar discs around Herbig Ae stars. The research will examine whether an increase in metallicity can cause the shadowed region of the disc to be irradiated, potentially leading to the formation of a flared disc, by analysing the extinction of stellar radiation.
Methods. A semi-analytical model was developed to study the temperature profile in the midplane of a circumstellar disc around a Herbig AE star. The model considers the transfer of 1+1D stellar radiation and heat dissipation through viscous processes and thermal conduction. Using publicly available data on gas opacities, the absorption of stellar radiation in gaseous discs with different metallicities was investigated and the resulting absorption was used to determine the temperature profile in the discs with various metallicities.
Results. The results showed that the temperature profile varies with metallicity, with higher metallicity resulting in a thicker gas disc that absorbs more radiation and leads to lower temperatures in the "dusty" regions of the disc. Additionally, increasing the metallicity caused the shadowed region of the disc to decrease and essentially result in a"flaring" disc.

Key words. Radiative hydrodynamic – Herbig Ae star – Dusty disc – Gas disc – Extinction

1. Introduction

The study of planet formation has undergone significant expansion in recent years due to the discovery of exoplanets and the availability of data on protoplanetary discs. Before this, our solar system was the primary test bed for planet formation models. The circumstellar discs of Herbig Ae stars have also gained significant attention as they were thought to contain clues about the formation process. However, it is well-defined that planetary systems around other stars are widespread and exhibit a range of configurations (Dong 2015). The initial circumstances and development of protoplanetary discs, where planets form, play a crucial role in shaping these characteristics. To better understand the structure and evolution of circumstellar discs, it is essential to use numerous tracers that can distinguish between diverse areas of the disc, such as gap generation by planets, dust growth, settling, and photoevaporation examine them at enormous scales (Baillié & Charnoz 2014). Despite these advances, there are still numerous unresolved questions regarding the origins of planets. The typical model for planet formation involves the gradual appearance of rocky planets from small dust particles, with some potentially gaining gas from the protoplanetary disc to become gas giants. Tsang (2014) demonstrated stellar insolation's role in forming gaps around massive planets in protoplanetary discs. The study's results suggest that the lack of low-metallicity eccentric planets in the "eccentricity valley" may be because this region is located in a shadowed area with no stellar illumination. This study emphasises how critical it is to consider stellar insolation when examining protoplanetary disc formation and structure. It is crucial to understand the hydrodynamic structure of circumstellar discs by taking into account stellar irradiation-induced heating and energy balance. To accurately model the amount of radiative cooling, it is crucial to accurately resolve the heating caused by radiative dissipation in the midplane of the disc. To further understand heat transmission within the disc, these models can be adjusted to include other heating sources, including viscous heating and thermal conduction (Schobert et al. 2019). Hydrostatic equilibrium occurs when the pressure and force gravity operating on a system is balanced. The state equation links the pressure to the gas density, temperature, and other factors. At the same time, gravity includes the system's self-gravity and the gravity from external sources such as a dark matter halo or a star. These considerations are essential for understanding the structure and evolution of circumstellar discs. The grains in diffuse interstellar medium differ from those in circumstellar discs, and the composition of dust particles in circumstellar discs can be estimated from millimeter continuous emission spectra(Sabri et al. 2014). A thorough understanding of dust characteristics and evolution is essential for understanding various attributes of circumstellar discs(Natta et al. 2007). A power-law distribution for the grain size is used to calculate the average maybe of dust particles, with the number density given by $n(a) \propto a^{-3.5}$ and a dust size distribution ranging from $0.005\mu m$ to $0.25\mu m$. The "Astronomical silicate" of Draine & Lee (1984) consists of $Mg_{1.1}Fe_{0.9}SiO_4$ with a density of $3.3gcm^{-3}$ and mean size $< a >= 1\mu m$. However, our limited understanding of dust grain behavior in dense clouds leads to uncertainties in the information we obtain about circumstellar discs. To address this, we have developed a new dust model

based on recent observations and research on dust in dense regions.

The structure of a passively irradiated circumstellar disc comprises three regions: an inner gaseous hole, a shadowed area (due to the vertical inner rim), and a flaring region (Dullemond et al. 2001). The vertical structure of circumstellar discs can be approximately calculated by solving the equation of vertical pressure along with an angle-dependent radiative transfer equation that uses approximations of Planck mean opacities. Our study demonstrated a numerical methodology to calculate the disc's midplane temperature and photospheric geometry using radiative hydrodynamics, including viscous dissipation and thermal conduction. Baillié & Charnoz (2014)'s investigated that shadowed regions appear at the boundary between diffusion-dominated zones, where viscous heating and thermal conduction dominate, and radiation-dominated regions. The model can be simplified by considering only diffusive heating, which is only valid when viscous heating is the dominant factor and depends on the surface mass density and viscosity. However, ignoring irradiation heating when studying the outer regions of the disc, where it is much more significant compared to viscous heating, limits the accuracy of determining the physical characteristics of the disc. By modeling circumstellar discs in a spherical coordinate system, it is possible to efficiently solve the Laplace equation (and accurately conserve flux) in a diffusive region and compute the integration of radiation along the optical path in the inner region (Schobert et al. 2019).

Various methods have been developed for determining the structure of a dusty disc, which previously involved directly solving the radiative transfer differential equation. These methods include using variable Eddington tensors, 5^{th} order Runge-Kutta integration, and 2^{nd} order finite differences. These approaches effectively solve one-dimensional problems and can produce accurate solutions, but they become more challenging for two- and three-dimensional problems (Jankovic et al. 2021; Whitehouse & Bate 2004).In this study, the accuracy of models was evaluated with "$1+1D$" radiative transfer and self-consistent surface density profile to calculate the vertical structure of the circumstellar disc (Dullemond & Natta 2003).

The dust sublimation radius was initially calculated by assuming geometrical extinction only (no absorption), which led to a puffed-up rim at dust sublimation temperature ($T_{sub} = 1500K$). However,Malygin (2016) observed gas opacity in a metallic gas disc had revealed significant differences in the extinction of stellar radiation under different metallicities when the gas equilibrium temperatures are higher than the local dust sublimation temperature. It is still not fully understood why there is a lack of molecular emission from gaseous discs, even though such emission is often seen in the surface layers of these dusty discs. There is evidence that the inner gaseous parts of discs around Herbig stars and around forming stars of higher masses are optically thick, and this plays a vital role in shaping the dusty circumstellar disc (Jankovic et al. 2021; Isella & Turner 2018). The absorption of gas is affected by its temperature and the radiation it is exposed. Hence the two-temperature Planck means must be employed to establish the equilibrium temperature in an optically thin gas. The total absorption, including line and continuum, is measured by the mean opacity for all species. The radiative cooling rate of an optically thin gas increases with temperature until a phase transition or radiative instability occurs, after which the excitation of gas molecules allows for more efficient cooling by releasing thermal energy. The Planck mean opacity measures the gas's transparency, dominated by continuum opacity, and its opaqueness, dominated by line opacity (Malygin 2016; Kuiper & Yorke 2013). The proper treatment of energy transport through circumstellar discs in developing more sophisticated hydrodynamical models relies on the accuracy of the opacity model and the computational power. The overall structure of the Planck mean gas opacities in a given system is determined by the interaction between continuum and molecular line opacities. Unless the temperature is so low that molecules are present, these mean opacities typically decrease as the temperature falls. The primary sources of both forms of mean gas opacities at high temperatures ($T > 6000K$) are continuum species, with scattering being the primary source at low densities. Depending on the density, the growth in molecular opacity species at intermediate temperatures ($3000K < T < 1500K$) causes an increase in both mean gas opacities. Mean gas opacities rise when molecular absorption takes over as the primary source of opacity at lower temperatures ($T < 1500K$)(Helling et al. 2000). At temperatures around 1500 K, the number densities of many molecules start to decrease, and more complex molecules like CH_4, NH_3, and CO_2 begin to appear. Still, there is insufficient data on their absorption and scattering properties to include them in calculations of line opacity. At lower temperatures, H_2, SiO, and H_2O are the primary opacity sources in both metal-rich and metal-poor environments (Helling et al. 2000).

Radiative transmission plays a significant role in understanding the physics of a disc as it can modify the density structure and affect the dust content and opacity through hydrostatic equilibrium. The temperature and survival of different dust grains can vary based on factors such as size, composition, and the inner edge of the disc, as demonstrated in previous studies Mathis et al. (1977). The model used in this manuscript incorporates temperature and density-dependent gas opacities from Malygin (2016) and frequency-dependent dust particle opacities fromDraine & Lee (1984). The physical structure of the circumstellar disc is based on the models of Malygin (2016) for the gaseous disc region and Dullemond Dullemond et al. (2001) and Schobert et al. (2019) for the dust disc region.

The structure of the paper is as follows. In section 2 delivers a basic mathematical terminology to structure of the disc and provides insight into heat transport interior to the disc. In Section 3 describes the influence of accretion heating on the equilibrium of gas disc and effect of extinction of photon on different metallicity. Section 4 presents different analytical solution of temperature profile interior to the disc due to metallicity. Section 5 explains a concept of different analytical errors and provide a conclusion.

2. Structure of the disc

In this section, We derive the mathematical solution governing the structure of dust discs with an inner hole. The disc is primarily heated by the radiation from the central star, which has a mass M_*, radius R_*, effective temperature T_*, and luminosity L_*. The plane-parallel 1+1D vertical radiative transfer equations are utilized to solve radiative transfer and vertical pressure balance. These equations are iteratively solved until convergence is achieved.

2.1. Radiative Hydrodynamics

The energy balance in protoplanetary discs comprises four components: radiative cooling, viscous heating, thermal conduction, and stellar heat flux. The model consists of two layers. The surface layer is directly exposed to direct stellar radiation, which radiates half of the absorbed radiation inward and the other half

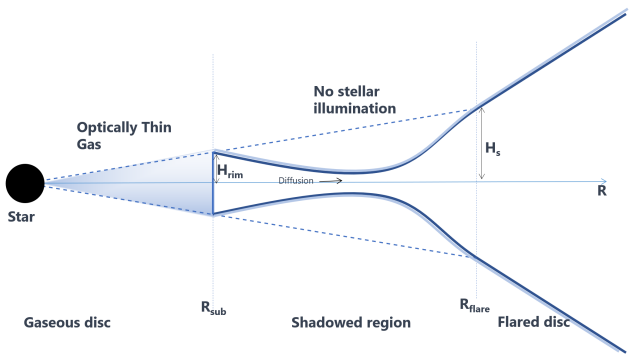

Fig. 1: The structure of a circumstellar disc around a Herbig Ae star, as described in Dullemond et al. (2001), consists of an inner hole filled with optically thin gas, a rim where dust condenses, a shadowed region where diffusive heating is dominant, and a flared outer disc.

into the atmosphere. The inner disc absorbs and re-radiates the radiation from the surface layer, causing the outer disc to be only heated to a small fraction of its optically thin radiative equilibrium temperature (Chiang & Goldreich 1997). These findings in the midplane of the disc are cooler (T <1500K) than its photosphere temperature. The disc geometry influences the impinging angle of the stellar radiation on the disc, which dictates how much energy is impinging onto the disc. This angle can be estimated by the vertical parallel-plane radiative transfer method (Dullemond, C. P. et al. 2002). Stellar radiation impinges onto the disc at an angle α can be approximated as

$$\alpha \approx \frac{0.4R_*}{R} + (\gamma - 1)\frac{H_s}{R} \tag{1}$$

The factor $(\gamma-1)$ is a gradually varying function that accounts for energy conservation.H_s is the height of the visible photosphere above the disc mid plane.If a circumstellar disc is irradiated at a given region with a positive grazing angle, it is possible that inner regions of the disc may cast a shadow over not irradiated region (Baillié & Charnoz 2014). The stellar flux impinging with this angle onto the disc is

$$Q_{irr} = \alpha \frac{L_*}{4\pi R^2} \tag{2}$$

where Q_{irr} is a stellar flux along the midplane. The equation assumes that the entire star is visible from the point on the disc surface because we are modeling a circumstellar disc with a large inner hole, allowing this assumption to be valid throughout the disc. However, in section 2.6, we will discuss situation where this assumption may not be valid. The temperature and density distribution of a dust disc can be determined by solving for hydrostatic equilibrium and local thermal balance in the vertical direction, starting with an initial guess for the grazing angle at a distance R. The surface density of the disc follows a power law. ($\Sigma \propto R^{-1.5}$), and the vertical density follows a Gaussian distribution if the disc is vertically isothermal with a constant pressure scale height given by

$$H_p = \frac{c_s}{\Omega_k} = \left(\sqrt{\frac{k_b T}{\mu m_H}}\right)\left(\sqrt{\frac{GM_*}{R^3}}\right)^{-1} \tag{3}$$

where c_s is the vertically isothermal sound speed and Ω_k is the angular velocity. The Virial temperature at the surface of the star is given by $T_c = GM_*\mu m_H/k_b R_*$, where T is the temperature in the midplane of the disc, G is the gravitational constant, $\mu = 2.3$ is the mean molecular weight of the gas (assumed to be a molecular hydrogen-helium mixture with a normal solar composition), m_H is the mass of a hydrogen atom and k_b is the Boltzmann constant. This equation describes the relationship between temperature, mass, and size in the central star and the surrounding circumstellar disc.The ratio of the photosphere height H_s to the pressure scale height H_p in a protoplanetary disc can be determined using equation (A9) from Dullemond et al. (2001), which assumes hydrostatic equilibrium:

$$1 - erf\left(\frac{\chi(R)}{\sqrt{2}}\right) = \frac{2\alpha}{\Sigma(R)K_p(T_*)} \tag{4}$$

Where $K_p(T_*)$ is the Planck mean opacity at stellar temperature T_*. The vertical structure of the disc, the distribution of gas, and the radiation within it can be understood by using this equation. Since the majority of the disc mass is below a few pressure scale heights, this approximation is reasonable. The disc's photospheric height (H_s) is defined as the point where the vertical optical depth of the disc to the stellar radiation is $\tau_z = 1$ on a ray from infinity. Stellar radiation impinges on the surface of a protoplanetary disc at a given radial position at an angle from the 1-D vertical plane-parallel surface. Half of this radiation is assumed to flow towards the disc midplane, increasing the optical depth in that region.

Before discussing the radiative transport in a circumstellar disc, it is crucial to consider the heating and cooling processes that occur within the dust particles within the disc. Understanding these processes can help us better understand how the star's temperature affects the opacity and, subsequently, the temperature of a dust particle. In the following subsection, we will discuss the Mie theory and how it relates to the behaviour of dust under different stars and the distribution of dust within the disc. However, this will not provide any insight into the midplane temperature profile (Dullemond 2012). The observational opacity characteristic of absorption and scattering efficiency of dust material was found to have the feature of silicate material. As a result and to simplify, a spherical shape with an "Astronomical silicate" composition was used to calculate the opacity of dust using Mie's theory (Vinković 2006).The opacity arises from the dielectric material's responses to the radiation's oscillating electric field. The dielectric material releases its electromagnetic radiation, interacting with the incident radiation field. This interference brings about absorption and scattering. The front of the particle cannot protect the interior from incident radiation if the particle is sufficiently smaller than the wavelength of peak emission. ($2\pi a/\lambda$) (Throughout the paper the grain size small enough to be in Rayleigh limit). Every particle reacts dielectrically to the incident field. However the silicate absorption feature at $10\mu m$ tends to constant $k_p(T_{dust}) \approx 1$(Jankovic et al. 2021).The absorption efficiency is calculated assuming it is independent of grain temperature and optically thin in the infrared wavelength, but our conclusion will remain unaffected (Laor & Draine 1993). The Planck mean opacity of stellar ($K_p(T_*)$) was calculated by assuming interstellar dust with spherical of fixed characteristic radius of $< a >$ (Setti & Fazio 1978). The "steady-state" grain temperature can be calculated by equating grain heating with photon absorption using the energy density of the interstellar radiation field and the wavelength-dependent grain absorption efficiency (Q_{abs}) with grain cooling (Q_{em}) by photon emission

$$\int_0^\infty \frac{\pi a^2 L_\nu}{4\pi R^2} Q_{abs}(m,a,\nu)d\nu = 4\pi a^2 \int_0^\infty Q_{em}(m,a,\nu)\pi B_\nu(T_{dust})d\nu$$

(5)

where $Q_{abs}(m, a, v)$ is the absorption efficiency, m is complex index of refractive index and $\pi B_v(T_{dust})$ is the Planck function for the dust temperatureDraine & Lee (1984).

$$\frac{L_v}{4\pi R^2} < Q(T_*) > \approx 4 < Q(T_{dust}) > \sigma T_{dust}^4 \tag{6}$$

The extinction cross-section (C_v^{ext}) is defined as the sum of the absorption (C_v^{abs}) and scattering (C_v^{scat}) cross-sections of grains in radiation transfer, and the extinction efficiency ($Q_v^{ext} = C_v^{ext}/\pi a^2$) is often used instead. The extinction of dust is much higher than gas, and the gas contribution to the coefficient can be ignored. The total extinction ($\sigma_v = nc_v^{ext}$) of a dust grain due to size distribution can be calculated by adding up the contributions of all of its components. The gram opacity (k_v) of dust, which measures the strength of the interaction between the dust and radiation field, is commonly used because the mass density of interstellar matter and the number density of grains are inversely correlated($k_V = \sigma_v/\rho_{dust} = 3Q_{abs}/4a\rho_{dust}$) (Preibisch et al. 1993). Radiative transfer is challenging to model as there is always a mixture of grain size, shape, and chemical composition. The dust is the primary source of emission and extinction of radiation. The silicate grain's sublimation temperature determines the upper limit of the Planck mean temperature, which may be representative of the temperature at the puffed rim($1500K$). The molecular cloud's temperature is in line with the lower limit ($10K$).

The photospheric height above the midplane of the disc can be estimated (using equation 1) if the assumed grazing angle is positive. Given the photospheric height is established, the irradiation heating term may need to be excluded from the equation for the midplane temperature because the disc column is not directly exposed to the star. The presence of shadowed regions within the disc, which receive little or no stellar radiation, is discussed in section 2.6. In section 2.6, there is a discussion of geometric refinements in the shadowed region.

2.2. Puffed rim

The interior of a circumstellar disc is typically made up of gas up to the sublimation radius, the distance from the central star at which silicate dust particles start to sublimate due to the high temperature. The density of silicate dust grains in an interior to the puffed rim ($T > 1500K$) is set to zero; thus, there are no dust particles in an inner region. It is often assumed that the gas interior to the rim is transparent to stellar radiation, so the influence of the gas on the disc structure is ignored, and the disc is treated as having an inner hole. However, in section 3, The effects of variations in the metallicities of the gaseous interiors with respect to the sublimation radii on the disc's optical thickness and structural design are explored. The vertical rim, exposed to direct stellar radiation, puff-up the inner rim since it is hotter than the flaring disc at the same radius (Chiang & Goldreich 1997; Pavlyuchenkov et al. 2022). Given the lack of knowledge regarding interaction (gas-dust coupling) and optical qualities at the phase transition, accurately describing the inner rim's vertical structure is challenging. The model mainly consists of amorphous silicate. The R_{rim} radius is determined by equating the emitted black body flux (σT_{rim}^4) to the received flux ($L_*/4\pi/R_{rim}^4$) from direct star radiation which essentially results in

$$R_{rim} \approx \left(\frac{L_*}{4\pi\sigma T_{rim}^4}\right)^{0.5}\left(1 + \frac{H_s}{R_{rim}}\right)^{0.5} \tag{7}$$

Where L_* is luminosity of star and temperature of the rim. The impact of self-irradiation is roughly explained by the factor $(1 + \frac{H_s}{R_{rim}})^{0.5}$. The vertical height of the inner rim, H_s is given by

$$H_s(R_{rim}) = \chi(R_{rim})H_p(R_{rim}) \tag{8}$$

Where H_p is the pressure scale

$$H_p(R_{rim}) = \left(\frac{T(R_{rim})}{T_c}\right)^{0.5}\left(\frac{R}{R_*}\right)^{0.5} R \tag{9}$$

and $\chi(R_{rim})$ is a dimensionless constant and usually lies between 2 and 6. The distance of dust evaporation in the midplane (R_{rim}) is computed at the point where $\tau_z = 1$, with a $(1 + \frac{z^2}{R_{rim}^2})$ geometric factor (arises from cylindrical coordinates.) that is very close to unity being neglected.The iterative process of solving equations 4, 7, 8 and 9 is continued until the relative ratio of H_{rim}/R_{rim} difference between iterations is below a certain threshold, typically set at 10^{-2}, to ensure convergence.

This puffed-up rim cast a shadow. The temperature rapidly drops below the inner rim of the disc to a temperature that is substantially lower than the temperature of optically thin dust at the same radius. However, radiative diffusion from the rim and viscous dissipation help to prevent cooling and prevent hydrodynamic collapse. The diffusive flux is inversely proportional to the temperature gradient and always has an outward component, which helps to maintain a stable structure in the disc (Dullemond et al. 2001)Schobert et al. (2019). The following subsection describes the various diffusive heating methods used to study radiation behavior within a circumstellar disc.

2.3. Viscous Dissipation

Viscous dissipation is due to the vertical gradient of the rotational frequency. It has been proposed by Hahn (2009) that vertical convection in a circumstellar disc may generate turbulence and thus be viscous through vertical motion. In the case of a passive circumstellar disc, the surface density profile remains constant over time, resulting in steady-state accretion. The magnitude of turbulent viscosity in such a system is parameterized using viscous-prescription $\alpha_{visc} = 10^{-2}$ proposed by Shakura & Sunyaev (1973), without making any assumptions about the specific source of turbulence. The presence of significant turbulent viscosity suggests that viscous dissipation must be considered in the energy balance Schobert et al. (2019). The viscous heating term Q_{visc}, can be derived from the Naiver-Stokes equation by taking the scalar product in spherical coordinate with the dominant azimuthal velocity field, which simplifies to

$$Q_{visc} = \rho v_t \left(R\frac{\partial\Omega_k}{\partial R}\right)^2 = \frac{9}{4}\rho v_t \Omega_k^2 \tag{10}$$

where is the $v_t = \alpha_{visc} H_p c_s$ kinematic turbulent viscosity and

$$\rho = \frac{\Sigma}{\sqrt{2\pi H_p^2}} \tag{11}$$

$\rho$is midplane density profile. The effect of viscous dissipation on the vertical structure and midplane temperature profile is discussed in section 3.2. The density profile calculated in equation 11 is only valid when there is a constant vertical temperature profile. However, this assumption is not strictly true because the

temperature profile does vary slightly along the vertical plane from the midplane. Despite this, the impact of assuming a constant vertical temperature profile is expected to be minimal because most of the disc mass is located at the midplane, resulting in a minor error in the temperature profile

2.4. Thermal Conduction

The effect of thermal conduction on the internal energy of a system is linked to the influence of momentum eddy diffusivity and heat transfer eddy diffusivity through the turbulent Prandtl number $P_r = 1$. The Prandtl number can be rearranged to derive the thermal conductivity (k_t)

$$k_t = \frac{\rho v_t \Gamma c_v}{P_r} \tag{12}$$

where Γ and c_v is adiabatic index and constant specific volume. The classical expression for thermal conductivity assumes a high-temperature gradient near the inner rim of the disc. It plays a significant role in the energy transport of hot gases in accretion discs, likely to operate under the collisionless regime. The turbulent thermal conduction in a spherical coordinate can be calculated using Schobert et al. (2019)

$$Q_{cond} = k_t \nabla T \tag{13}$$

Additional heating sources, such as viscous, thermal conduction, and radiative cooling, may produce a new midplane temperature profile. The effect of thermal conduction on the vertical structure and midplane temperature profile is discussed in Section 4.2.

2.5. Radiative cooling

Accurately determining the energy balance and midplane temperature of a circumstellar disc requires considering various cooling mechanisms, with radiative cooling from the disc surfaces being the most important. The local heating rate from internal processes, such as viscous, thermal, and radiative heating, determines the rate of radiative cooling at each point in the disc. The vertically integrated heating term Q_{heat} equation reads

$$Q_{heat} = \Psi_s \left(\frac{1}{2} Q_{irr} + Q_{visc} + Q_{cond} \right) \tag{14}$$

The radiative losses from the surface are denoted by the cooling term Q_{cool}, which is written as

$$Q_{cool} = \Psi_i \sigma T^4 \tag{15}$$

The dimensionless quantity Ψ measures the interaction between the disc‘s radiation and external radiation. Ψ_s considers the possibility that the disc‘s interior is not fully optically thick to the emission from the surface layer, while Ψ_i measures the possibility that the internal disc is not fully optically thick to its radiation (Dullemond et al. 2001). The temperature interior to the disc is calculated assuming $\Psi_s = \Psi_i = 1$. In other words, the calculation assumes that the disc's interior is fully optically thick to both the surface emission and its radiation. The disc's temperature determines the emitted flux from a vertically isothermal disc. The disc is always in hydrostatic equilibrium. To accurately calculate the midplane temperature profile of a circumstellar disc, an iterative process involves equating equations 14 and 15 and continuing until the relative temperature difference between iterations is below a certain threshold, typically set at $\frac{T_{new} - T_{old}}{T_{old}} < 1$. This helps to ensure convergence and accurately determine the disc's temperature distribution without the need for intensive computational power.

2.6. Shadowed region

The puffed-up rim intercepts the stellar radiation. As a result, this casts a shadow on the outer disc, and the temperature behind it drops substantially lower than the optically thin dust at the same radius. The radiative diffusion from the rim and viscous heating prevents the shadowed region from cooling and collapsing. The disc flares, emerging from the shadow at a large distance and re-emerging to stellar heating (Zhang et al. 2021). The flaring radius (R_{flare}), at which the surface of the disc is illuminated again by stellar radiation, can be calculated using similar triangle properties, $\frac{H_{rim}}{R_{rim}} = \frac{H_s}{R_{flare}}$ (to visualize, see Figure 1). To calculate the temperature profile and vertical structure in the shadowed region of a circumstellar disc, it is necessary to equate equations 14 and 15 without considering the irradiation term Q_{irr} (no stellar illumination) (Dullemond et al. 2001; Dullemond, C. P. 2002; Bell 1999).

3. Structure of the gaseous disc

The stellar radiation into gas with enough energy to exceed the gravitational potential causes the disc gaps to open. The surface density of the gas disc follows a power law ($\Sigma \propto R^{-1}$) similar to a dusty disc. The condition of hydrostatic equilibrium determines the vertical profile of gas density in the inner hole region. The gas pressure sustains the optically thin disc (Armitage 2015; Chiang & Goldreich 1997). Tsang (2014) demonstrated how stellar illumination/insolation could influence gaps forming around massive planets in cold discs. The research also suggests that the lack of low-metallicity eccentric planets in the "eccentricity valley," a region where planets are not observed to exist, can be explained by the fact that this reason is located in a shadowed region where there is no stellar illumination. The eccentricity distribution of metal-reach and metal-poor samples is similar beyond 1AU, where they are now visible; planet formation may have occurred without the need for a vast, densely packed planet (may have exchanged their angular momentum). With increasing the metallicity, the gas disc becomes optically thicker, preventing direct insolation from puffing up the dust rim and potentially resulting in the shadowed region disappearing (Tsang 2014). To study the effect of metallicity on the extinction characteristics of gas, Semenov, D. et al. (2003) kept the absolute amount of metallic iron in silicates constant and produced "iron-rich," "normal," and "iron-poor" models.

3.1. Equation of state

The radiation hydrodynamics in a gaseous disc are modelled using the ideal gas equation of state, where the pressure (p) is related to the gas temperature (T_{gas}) and density (ρ) through the pressure equation $p = k_b \rho T_{gas} / \mu m_H$. The energy exchange between the radiation and gas fields depends on the relative temperatures, gas density, and gas opacity Malygin (2016)'s work provides more information on how the radiative transfer process is implemented, including the interpolation of the (Semenov, D. et al. (2003)) opacity table to determine gas opacities for different metallicities.

3.2. Radiative Transport

The radiative transfer problem involves the emission, absorption, and transport of photons in a gaseous disc, which an equation along a straight line in a radial plane can represent. The equations describe the movement and absorption of primary photons

as they radiate outward from the star and are absorbed by gas molecules in the gaseous disc. An Equation 15 (radiative cooling) describes the initial temperature profile of the disc and is expected to be that of an optically thin gas. Therefore, it is anticipated that the initial temperature of this region will be similar to that of an optically thin gas. The temperature of the gas can be calculated by assuming that it is in radiative equilibrium with the radiation field as the only source of energy and in local thermodynamic equilibrium. This can be done by solving the implicit equation for thermal emission:

$$F_{irr} = \frac{L_*}{4\pi R^2}(1 + \frac{H}{R_{rim}})exp(-\tau(R)) \quad (16)$$

where Planck mean optical depth $\tau(R)$ (along the radiation transport) is defined as

$$\tau = \int_{R_*}^{R} kp(T_*, T_{gas})\rho_{gas}(R)dR \quad (17)$$

where $kp(T_*, T_{gas})$ is the gas absorption opacity (cm^2g^{-1}). The sublimation radius determined in section 2.2 is an upper bound based on the assumption that dust grains at the puffed-up rim absorb all unabsorbed radiation from the star. In the absence of absorption, the molecular line opacity will be low and independent of the gas temperature. If we consider that some of the stellar energy is absorbed, it can be shown that the outer distance decreases by a factor of $e^{-\tau}$ for small optical depth. The term $\frac{L_*}{4\pi R^2}$ corresponds to the geometrical attenuation along the radially outgoing direction. The factor $(1 + \frac{H}{R_{rim}})$ accounts for the effect of self-irradiation on the rim. In the following subsection, the absorption of photons from the star in the inner region is influenced by the gas mean opacity $kp(T_*, T_{gas})$, which is determined by the local gas temperature and the photosphere temperature of the star. The gas mean opacity, in turn, determines the equilibrium temperature in an optically thin gas.

3.3. Equilibrium temperature

The two- temperature Planck means were necessary to calculate the radiative equilibrium since radiation and gas temperatures are different. The Planck mean opacities were computed using Malygin, M. G. et al. (2014)'s data sets while assuming local thermodynamic equilibrium of an equation of state. The data consist of broad range of stellar temperature $(3,000 - 1,00,000)K$, gas temperature $(700 - 10^6)K$, gas densities $(10^{-20} - 10^{-2})gcm^{-3}$, gas pressure and for three different metallicities $[Me/H] = -0.3, 0, 0.3$.The absorption of radiation by the gas is influenced by the gas Planck mean opacity $kp(T_*, T_{gas})$, which depends on both the local gas temperature (which determines its chemical abundance and composition) and the radiation temperature. Given the gas temperature is lower than equilibrium temperature ($T_{gas} < T_{eq}$), the gas temperature will be heated to the equilibrium temperature. Conversely, if gas temperature is greater than the equilibrium temperature ($T_{gas} > T_{eq}$), the gas temperature will be effectively cooled down to the equilibrium temperature.The condition for the equilibrium temperature can be determined using equation 9 from Malygin, M. G. et al. (2014), which assume negligible extinction

$$T_{gas} = \left(\frac{\kappa_P(T_{gas})}{\kappa_P(T_{gas}, T_{rad})}\right)^{-1/4} \left(\frac{R_*}{2R}\right)^{1/2} T_* \quad (18)$$

The first term $\kappa_p(T_{gas})/\kappa_p(T_{gas}, T_{rad})$ describe the emissivity of the gas. The emissivity of the gas changes with temperature and is affected by the non-equilibrium chemistry of gas species. The relative abundance of certain species can be altered by equilibrium chemistry, leading to significant variations in opacity in the radial plane (Malygin, M. G. et al. 2014). The density is calculated using the ideal gas law and the appropriate chemical mixing ratio (Isella & Turner 2018). The second term $(R_*/2R)$ corresponds to the geometrical attenuation along the radially outgoing direction. The non-monotonic behavior of the ratio of the two-temperature Planck opacity as a function of temperature and density can introduce multiple solutions for the equilibrium gas temperature without the need to solve for radiative transfer.

3.4. Metallicity

The lack of molecular emission observed in gaseous discs remains an open question in astrophysics. One possible explanation is the presence of different chemical cycle processes in different metallic environments, which may depend on the system's metallicity. It has been proposed that a lower metallicity can increase the temperature of the gaseous disc, resulting in changes in the efficiency of chemical reactions that form and destroy various species. This can lead to an overabundance of certain gaseous species, such as CN, CO, HCO^+, and N_2H^+, which may be more easily detectable in low-metallicity environments (Drummond, B. et al. 2018). The mean opacity of the gas is influenced by temperature and species. As the temperature drops radially outward, the thermodynamic conditions change, and the opacity also decreases. At high temperatures ($T_{gas} > 6000K$), the mean opacity is primarily caused by atomic metal absorption (continuum species). In the intermediate temperature range of $6000K - 1500K$, the mean gas opacity increases with number density and is caused by continuum species. At $T = 1500K$, the number densities of most line opacity molecules start to decrease, while complex molecules such as CH_4, NH_3, and CO_2 are present, but continuum absorption is due to H_2^- and CO (Molecular opacities) (Malygin, M. G. et al. 2014; Fontes 2015; Helling et al. 2000).

The mixing timescale for gas in the inner region of a disc is long, and dust replenishment is slow, leading to a zero number density of silicate. This makes the inner region optically thin due to the dominant opacity sources being free-free and Compton scattering. While inside the "dusty" disc, the primary sources of opacity are bound-free and bound-bound interactions (Fontes 2015). The equilibrium of photoelectric heating and fine structure line cooling of neutral oxygen determines the gas's temperature. Dust heats and cools continuously, whereas gas heats and generally cools at discrete wavelengths (line absorption/emission), with a few exceptions, such as H. The presence of metals in the gas can significantly affect the opacity at high and low temperatures. At high temperatures, metallicity affects atomic absorption (and contribution to opacity), while at low temperatures, the formation of compound composition (the change in opacity is due to scattering and absorption). The opacity is dominated by bound-free, hydrogen-bound-bound and free-free absorption and is insensitive to metallicity (Gehrig et al. 2022). The metallicity affects the Planck mean differently at different temperatures.

3.5. Correction to Puffed rim

The gas density of the inner disc can be derived from the value of the dust surface density, assuming the abundances of certain grain species are known. The low gas density allows for the

formation of an optically thick rim (Benisty, M. et al. 2010). The grain abruptly destroyed at $1500K$ would transition from high dust opacity on the low-temperature side to molecular(gas) opacity on the high-temperature size (Calvet et al. 1991). The total opacity diminishes as the number of metals (metallicity) is reduced, but the condensation temperature also reduces since fewer metals are available (Ferguson et al. 2005). Direct star radiation travels spherically and exchanges significant outward momentum with gas molecules when absorbed instantly outside the dust sublimation front in the region where there is no dust. The temperature in this area is low because neutral gas has significantly lower opacity than dusty or ionized gas. The gas opacity (dust-free region) plays a vital role in shaping the circumstellar disc(Malygin, M. G. et al. 2014). The photoevaporation rate of a disc decreases with increasing metallicity due to the effectiveness of dust shielding in preventing photons from heating the rim. This leads to lower temperatures and a smaller vertical height of the rim.The decrease in the height of the rim, effectively reduces the shadowed region. At lower metallicities, photoelectric heating becomes less efficient, resulting in a significant drop in the photoevaporation rate. Low metallicity systems may have optically thin gaseous discs and higher flux at the rim, resulting in higher temperatures and a larger vertical height for the rim. The larger vertical height of the rim, effectively increases the shadowed region. (Nakatani et al. 2018).

4. Results

This section presents the effects of different metallicities on the vertical rim height and sublimation radius. The influence on the vertical structure and midplane isothermal temperature profile due to diffusion and irradiation heating sources in different regions is also described.

The model computes the physical structure of a passive circumstellar disc between the inner radius at the dust sublimation radius $R_{rim} = 0.52AU$ to the outer radius of 100 AU of a typical Herbig AE star with mass $M = 2.4M\odot$, radius $R = 2.4R\odot$, effective temperature $T_{eff} = 9500K$ and luminosity $L = 47L\odot$ (Dullemond et al. 2001).The minimum mass solar nebula surface mass density model of the solar protosystem, described by Crida (2009) and Ayliffe & Bate (2009), is given by

$$\Sigma(R) = \begin{cases} \Sigma_g (R/AU)^{P_1} & R_* < R < R_{rim} \\ \Sigma_d (R/AU)^{P_2} & R_{rim} < R < 100AU \end{cases} \quad (19)$$

The surface densities of the gaseous and circumstellar discs were found to follow self-similar power laws with exponents of $p_1 = -1$ and $p_2 = -1.5$, respectively. The inner region of the disc was characterized by a steep density gradient, while a shallower density gradient represented the outer region. The surface density constants were determined to be $\Sigma_g = 5g/cm^2$ and $\Sigma_d = 2000g/cm^2$ based on the normalized densities at 0.1 AU and 1 AU in the respective discs. It was found that the specific expression of the surface density constant did not significantly impact the overall findings of the analysis of the distribution of gas and dust in the disc. The model assumes dust and gas are fully coupled with a density ratio of 1:100, respectively, and the star is treated as a point source. The model used in this manuscript incorporates temperature and density-dependent gas opacities from Malygin (2016) and frequency-dependent dust particle opacities from Draine & Lee (1984). For our calculation of 'Astronomical silicate' with density 3.3 gcm^{-3} and mean dust's radius distribution of $1\mu m$ used to derive emissivity of dust grain.The Planck mean opacity of the dusty disc material, when exposed to the radiation from the stellar source, was calculated to be $kp(T_*) = 1939.50cm^2g^{-1}$.However, the temperature profile of the disc appears to be independent of its own radiation, as described in section 2.1.

4.1. Circumstellar disc structure

The initial focus of the model is on the existence of a puffed-up inner rim near the dust sublimation radius and the role of energy conservation in considering the shadow cast by the rim onto the disc.The circumstellar disc's surface height and pressure scale height are plotted on a logarithmic scale with 256 grid cells spaced linearly in Figure 2. The vertical height in the shadowed region beyond the puffed rim decreases rapidly beyond 0.47 AU. The surface height in the shadowed area is determined by diffusive terms in the range of 0.47 AU to 1.3 AU from the inner edge to the outer edge. The inner edge of the shadowed region and the puffed-up rim initially have a sharp temperature differential, which leads to thermal conduction from the rim defining the disc's surface height.The effectiveness of thermal conduction on disc structure is demonstrated later in this section. The initial vertical structure is shown in Figure 2 is the height of the puffed-up rim, which is calculated using the nonlinear Newton-Raphson method. This method involves solving multiple equations (4(χ),7 (R_{Rim}),8(H_s) and 9 (H_p)) simultaneously and iterating the equations until the ratio of $(H_{s,old}(R_{rim}) - H_{s,new}(R_{rim}))/H_{s,old}$ converges to less than 10^{-2}. The value of $\chi = H_s/H_p$ parameter can influence by various factors, which characterize the distribution of the material in a disc and affects the shape of the disc behind the rim, which is between 2 and 6, as stated in (Dullemond et al. 2001) and contradicts the Chiang & Goldreich (1997) that the chi ratio is radially uniform.

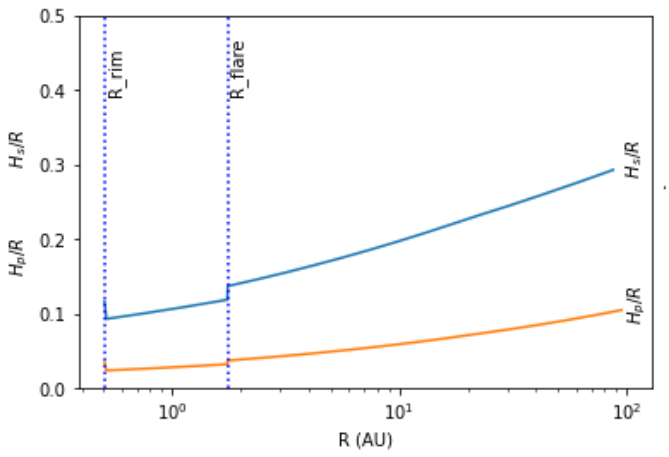

Fig. 2: The photospheric height of a disc is the height at which the optical depth in the vertical plane from infinity reaches a value of one. The disc is assumed to be in vertical hydrostatic equilibrium, with a scale height above the midplane determined by the local temperature of the gas, which can be influenced by diffusive heating and stellar irradiation. The vertical axis in this graph represents dimensionless quantities, while the horizontal axis represents radial distance in astronomical units (AU) units.

The shadowed region in the model was originally constructed without considering the influence of viscous heating or thermal conduction, based on Dullemond et al. (2001)'s modeling assumptions. To more accurately reproduce the vertical

structure in a hydrostatic simulation, viscous heating was included in the energy balance. Thermal conduction was also included in the model to account for the effect of turbulent heat transfer, which is essential for momentum transfer and cannot be ignored when analysing the temperature profile based on the Prandtl number $Pr = 1$ Schobert et al. (2019).The shadowed length was determined using the ratio of scale height to radial distance in relation to the flaring radius using a similar triangle. The shadow encompasses all points on the disc up to the flaring radius ($R_{shadow} = R_{flare} - R_{Rim}$), which has a radius of $H_s/R = H_{Rim}/R_{Rim} = 1$. The addition of diffusive heating decreased the shadowed length from 1.99 AU to 1.26 AU.

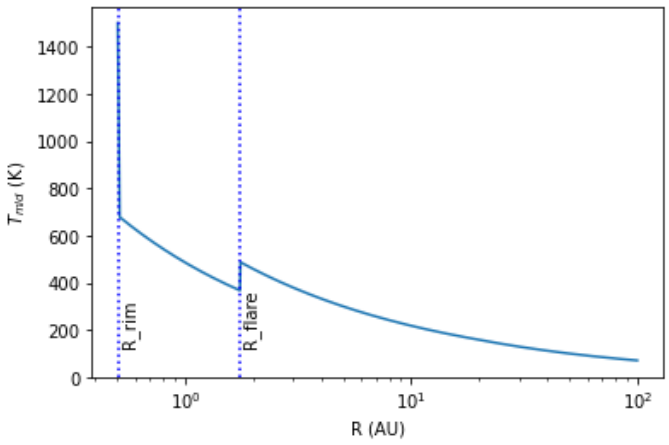

Fig. 3: The midplane temperature profile in a Herbig AE disc is primarily controlled by diffusive heating in the shadowed region and by 1+1D radiative transport in flared region. In the flared region (above 1.3 AU) of the disc, the temperature profile follows a power law of T $\propto r^{-1/2}$, indicating that these regions are dominated by direct irradiation from the central star.

The circumstellar disc temperature profiles in Figure 3 were created by averaging the midplane gas temperature using a 1+1D radiative transfer mode. The resulting temperatures in the circumstellar disc typically range from sublimation temperature 1500K to ambient temperature of 30K, higher for grains with lower opacities. The initial temperature profile of the disc is influenced by different heating modes, with the outer regions dominated by irradiation heating and the innermost regions primarily affected by viscous and conduction heating through diffusion. The effect of viscous dissipation on the vertical structure of passive disc were calculated assuming constant accretion rate of $2 \times 10^{-7} M_{\odot} yr^{-1}$ and viscosity parameter $\alpha_{viscs} = 0.01$. The inner edge of the shadowed region and the puffed-up rim initially have a sharp temperature differential. This sharp temperature change results in a significant gradient, making it harder for diffusive heating to converge. The shadowed region has a less steep radial variation in temperature due to its diffusive nature resulting in being slightly cooler than the flared region. The iterative process of solving the equations is continued until the relative temperature difference between iterations is below a certain threshold, typically set at 1, to ensure convergence. A power law $T(R) \propto r^{-0.50}$can be used to model the temperature profile with radial distance, consistent with the assumption of a steady state and the flared outer disc model. Dullemond et al. (2001) predicted a smooth curve in the temperature profile, including right behind the puffed rim. A smooth curve in the temperature profile indicates appropriate heat transfer between consequent grids, while a sudden change in the temperature profile may indicate an unstable system. This may be due to an inability to find the appropriate grid length to resolve the initial large gradient (Rapid temperature reductions occur with a vertical scale that is significantly smaller than the grid's thickness.) using constant initial boundary condition(1500K).The potential presence of shadowing effects can lead to numerical instability, which can be resolved by increasing the radial resolution (or use adaptive mesh refinement). However, this resolution increase may also increases the risk of computational instability (Baillié & Charnoz 2014) and require longer computational times. A sudden change or spike in the temperature profile may be more challenging to interpret and may require further investigation to understand its causes and implications.

The temperature profile of the disc is shown in Figure 3, with the midplane being colder than the surface due to its indirect heating by reprocessed radiation and its direct shielding from stellar light. The temperature rapidly decreases below the inner rim to lower levels than the temperature of optically thin dust at the same radius(Dullemond, C. P. 2002). The rest of the disc is much cooler than the inner rim, directly exposed to the star's radiation field. The disc's outer edge exhibits a typical flare, which can be identify by the kink (sudden jump) in the temperature gradient. The relative height of the kink in the temperature gradient (H_s/R) increases with radius, indicating that the height of the disc's surface rises faster than its radius, which is how flares typically appear.

The temperature and density of the entire disc were determined through an iterative process, in which the flaring index $FI = \frac{H_s}{H_{rim}} \frac{R_{rim}}{R}$ was recalculated after each iteration to ensure that the flaring angle was consistently calculated. The midplane temperature and midplane density were then determined once the iteration process had converged, using the height above the midplane at which direct stellar radiation is extinguished ($FI > 1$) to estimate the surface height of each annulus (Dullemond & Natta 2003).In this study, we examined the properties of rims in discs with low surface densities, assuming that the rims are formed by the evaporation of silicate dust particles of size $1\mu m$. We found that the surface density of silicate dust is 10^{-14}, while the density of Benisty, M. et al. (2010) is 10^{-11}. These differences in density measurements are due to the different treatment of gas and dust opacities and the simplification of radiative hydrodynamics in 1+1D structures. We discover that a low-density region is consistent with the location and characteristics of the rim.

4.2. Gaseous disc structure

The sublimation radius was previously computed in section 4.2, assuming that stellar radiation is not absorbed in the gaseous disc. Observations of the discs surrounding Herbig stars have revealed the presence of optically thick gaseous clouds within the sublimation radius (Isella & Turner 2018).To study the effect of metallicity on the gaseous disc and it is absorption coefficient at the sublimation radius, its necessary to determine the gas equilibrium temperature in an optically thin gas. This is because the transport of stellar radiation along the radial plane in the gaseous disc is absorbed by gaseous molecules, and the absorption rate depends on the metallicity of the gas. The Malygin, M. G. et al. (2014) publicly available data consists of measurements of metallicity $(-0.3, 0, 0.3)$, stellar temperature $(3000 - 30,000K)$, gas temperature $(700 - 10^6 K)$, density (gcm^{-3}) and pressure $(10^{-20} - 10^{-2} gcm^3)$ in a dusty circumstellar medium. These parameters have been calculated using an ideal gas equation and a

chemical equilibrium model based on local thermodynamic conditions. The data includes two variations of the Planck model, which represent different assumptions about the temperature of the gas relative to stellar temperature. The "two-temperature" Planck model is necessary for accurately modeling the balance of energy due to radiation in low-density gas in the circumstellar environment (Gilman 1974).

The radial temperature profile of a gaseous disc exhibits three distinct regions. The innermost region is directly heated by starlight and is composed of a gaseous disc. The vertical puffed rim of the disc is protected from direct radiation due to the presence of gas, which also contributes to the overall opacity of the disc. The synthesis of complex compounds in this region can be influenced by the star's metallicity, with higher metallicity resulting in a thicker gas disc and lower flux at the rim, leading to lower disc temperatures and a smaller vertical height for the rim (as suggested in equation 16). In contrast, lower metallicity disc have a higher flux at rim, resulting in higher disc temperatures. In general, the temperature of the disc is controlled by the star's irradiation, with lower metallicity stars leading to higher disc temperatures. The temperature profile of a disc around a star

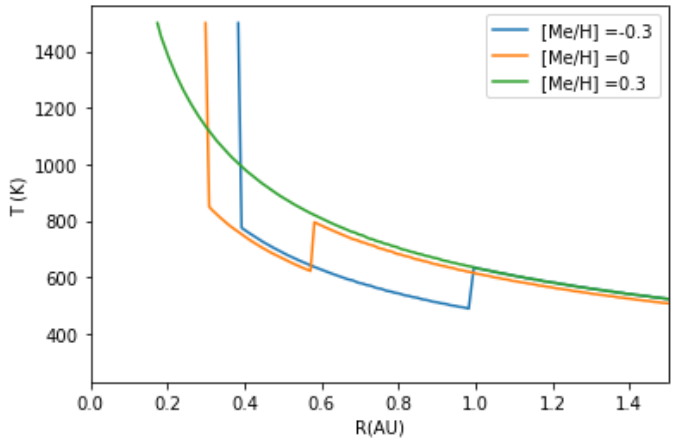

Fig. 4: The metallicity of a gaseous disc is expressed as the atomic abundances of all species except for H and He. The temperature profile of the disc can vary depending on the optical depth (/metallicity) along the radial, as illustrated by the three colored lines in the plot. These temperature profiles were calculated using the same initial grain distribution described in a section 2.1

was observed to vary with metallicity, as shown in Figure 4. The disc with a metallicity of 0.3 displayed a flared vertical profile, characterized by a lack of a kink in the temperature profile. In contrast, the temperature profiles of discs with metallicity values of -0.3 and 0 were similar but shifted along the radial plane. This similarity is likely due to the initial boundary condition of thermal conduction, which generally produces a similar initial temperature profile. Although the temperature profile depends on the radial position of the sublimation radius, the slight difference in sublimation radius (0.017 AU) between discs with metallicity values of -0.3 and 0 did not significantly affect the temperature profile. The temperature profile above 1 AU is same for different metallicity (similar to Tsang (2014)'s finding). However, it is expected that increasing the metallicity will result in a decrease in the dust-to-gas ratio, leading to concentrated midplane density profile and potentially a different temperature profile.The dust composition, size distribution and slope of the dust size distribution were identical across all metallicities.However,this may be an oversimplification as the process of dust growth in different metallic environment is still poorly understood (Drummond, B. et al. 2018). These findings suggest that metallicity plays a role in determining the temperature profile of a circumstellar disc, but other factors such as the initial boundary (type of dust material) condition of thermal conduction and the distance from the star are also important. In the present model, the dust-to-gas ration is kept constant at 1:100, which may be the reason for observed similarity in the temperature profile beyond the shadowing region.

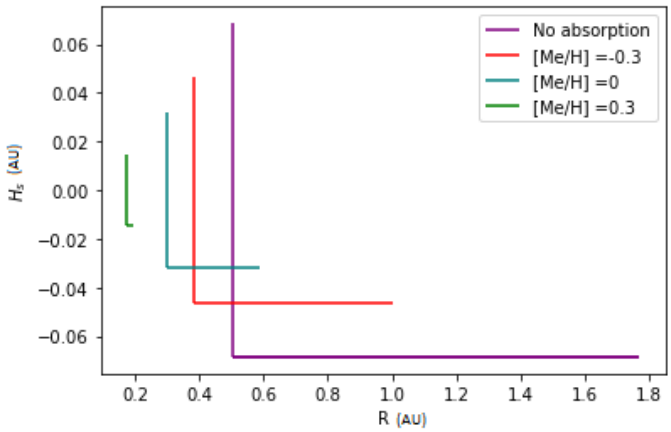

Fig. 5: The sublimation radius was determined using Planck's mean opacity, as described in section 3.2.The plot illustrates the variation of the sublimation radius, the vertical height of the puffed rim, and the length of the shadowed region for different metallicities, as indicated by the different colored lines. The position of the sublimation radius is represented by the position of the vertical line, the size of the vertical line represents the height of the puffed rim, and the length of the horizontal line represents the length of the shadowed region.

This study analysed the sublimation radius (R_{rim}) and vertical height (H_{rim}) concerning metallicity. The sublimation radius is the radius at which the optical depth along the midplane measured from the infinity reaches one. At the same time, the vertical height is the height at which the optical depth in the vertical plane from infinity reaches one. Using a geometrical extinction assumption, the original values for the R_{rim} and H_{rim} were determined to be 0.47AU and 0.06AU, respectively.The vertical height and shadowed length of the disc were calculated using the gas Planck's mean opacity, as described in sections 2.2, 3.2 and 3.3. The temperature of the gas at the sublimation radius was determined through an iterative solution, using the "LinearNDInterpolator" python module to calculate the opacity values. The results showed that increasing metallicity causes the disc's optical thickness to increase, with optical depth at the rim values of 0.91, 0.81, and 0.75 for metallicity values of -0.3, 0 and 0.3, respectively. This leads to a reduction in the amount of stellar flux reaching the rim. The sublimation radius was found to be $R_{rim,[Me/H]} = 0.38AU$, 0.29 AU, and 0.17 AU for metallicity values of -0.3, 0, and 0.3, respectively. The corresponding vertical heights were $H_{rim,[Me/H]}$ = 0.046 AU, 0.032 AU, and 0.019 AU. The difference in sublimation radius is due to the amount of stellar energy absorbed by the rim (as explained in section 3.2 and 2.2), while the change in vertical height is due to the change in pressure scale height as described by equation 9. The reduction in vertical height leads to a smaller shadowed length, which was found to be shadowed length = 0.62 AU,0.29 AU, and 0.12

AU for metallicity values of -0.3, 0, and 0.3, respectively. It was found that when there is no absorption in the gaseous disc, the calculated shadowed length is more than double that of a disc with a metallicity of -0.3 (the lowest value being examined). The shadowed region of a "no absorption" disc was found to be 1.266 AU, while the shadowed region of a disc with a metallicity of -0.3 was 0.62 AU. This suggests that it is important to consider the presence of a gaseous disc, even if it is optically thin, when calculating the properties of a circumstellar disc.

The shadowed length values correspond with the metallicity values and can be visualized using similar triangles (as shown in Figure 1).

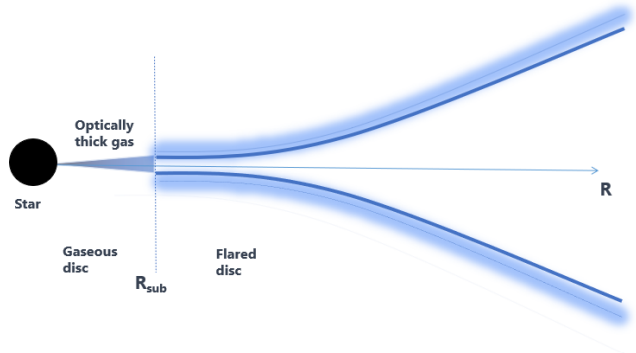

Fig. 6: The gas within the sublimation radius of a star has an increased optical thickness due to increase in metallicity. This is due to the dominant presence of molecular lines, specifically H and He, which increase the gas's opacity. As a result, the stellar flux at the rim is reduced and the shadowed region is eliminated.

Despite the calculation of a metallicity of 0.3 indicating a shadowed length of 0.12 AU, the temperature profile shown in Figure 4 does not show a kink in the gradient. This may be due to the resolution of the grid, which is 0.2 AU, being larger than the shadowed length. It is possible that the shadowed length falls within the boundary of the grid, or that the dominance of diffusive heating is similar to that of a flared disc. Further investigation may be necessary to understand the cause of this discrepancy. The gas within the sublimation radius of a star has an increased optical thickness due to its higher metallicity. The circumstellar disc exhibits flaring behavior similar to that shown in Figure 6 with increasing metallicity.

5. Discussion

Although the circumstellar disc is a complex 3D structure, modeling radiative transport, chemistry equilibrium, and thermal balance would be time-consuming. The 1+1D model simplifies this process by only considering radiation transfer in the vertical direction (without requiring radiation to follow the shortest path over the disc's surface) (Henning et al. 1996) (Jonkheid et al. 2004).

A significant source of uncertainty is the lack of knowledge about the detailed structure of the inner disc region. The calculation of the disc truncated at the dust sublimation radius and puffed up due to exposure to direct stellar radiation. The structure of this puff-up rim is very complex to model, depending on the detailed 1+ 1D radiation transport effects on the structure of the disc (Habart, E. et al. 2004). Including the density dependence of the sublimation, temperature allows the model to be precise by giving the rim front in a disc a rounded form. (Flock et al. 2016).In our model, we assume that dust evaporates independently of its density. However, it is important to note that in reality, dust is made up of different materials that evaporate at different temperatures.

Synthesizing dust grains in the laboratory, known as cosmic dust analogues, is essential for studying the characteristics of dust grains in different astrophysical environments. These dust grains can be produced using pulsed laser ablation and gas-phase condensation. Pulsed laser ablation involves vaporizing a silicate or metallic target using a laser and allowing the vaporized atoms, molecules, and clusters to condense at a pressure of 3 mbar in a quenching gas environment, resulting in the production of nanometre-sized silicate particles (Sabri et al. 2014). The tiny particles that make up interstellar silicate may exhibit different optical properties due to collective processes. Still, small amorphous grains are expected to have the same properties as bulk material because they only show non-collective phenomena. Cosmic dust analogues can be used to study dust's condensation and interstellar silicate properties (Henning et al. 1983).Sabri et al. (2014).

The Dullemond et al. (2001) model assumes that the dust and gas in a disc are fully coupled and their temperatures are equal, but this assumption may not hold in certain circumstances, such as near the disc's surface (Dullemond, C. P. et al. 2007). The thermal coupling between the gas and dust influences the gas's temperature in the disc's upper layers. However, this model ignores this coupling. The rate of collisions between gas molecules in the optically thin regime is often higher than the rate of coupling between dust and gas, resulting in the gas contributing to the high opacity of the disc Malygin (2016). The dust absorbs more radiation than the gas and is strongly heated by the star, leading to a thin boundary between vapor and condensed dustSchobert et al. (2019). The gas and dust in a protoplanetary disc generally have different temperatures, but the gas is able to quickly adjust to the temperature of the dust, resulting in similar temperatures for both. The impact of the difference in gas and dust temperature on the final temperature is therefore relatively small and can generally be ignored Jonkheid et al. (2004).

Scale heights have been seen to decrease with decreasing grain opacity due to the enhanced radiative cooling that can happen at lower opacities, resulting in cooler and flatter discs. The lowest grain opacity state, where gas and radiation may decouple and lessen the effectiveness of radiative cooling, is an exception to this trend. The "astronomical silicate" dust grain is considered homogeneously spherical and has a mean distribution of $1\mu m$. Still, its scattering may be non-isotropic, potentially leading to lower temperature structure errors despite being believed to be isotropic (Draine & Lee 1984).

The dust in the disc must release thermal radiation as a result of energy conservation. This infrared light may be absorbed and re-emitted by the disc multiple times, depending on the optical depth of the disc, before finally escaping to infinity. However, the radiative diffusion process allows the radiation to penetrate the disc entirely and ensures that the temperature is thoroughly determined at every location, regardless of the optical depth (Dullemond, C. P. 2002).

The disc's interior is only heated by radiation from the surface layer that diffuses downward without considering the radial radiative transfer process. It is unclear why, in this scenario, the disc will always flare (and emerge from the shadow) at radii where it can. The flared portion of the disc contracts and returns to the shadow when it is artificially cooled and remains shadowed (Dullemond, C. P. 2002).

The shape of the shadowed region depends on secondary heating sources like rim heating and viscous heating (Rodenkirch, P. J. et al. 2020). The drop in temperature in the shadowed region is often misinterpreted as a depletion of density (Isella & Turner 2018). Turbulence caused by viscous accretion can lead to diffusion of dust particles, and additional heating sources such as viscous and thermal conduction, as well as radiative cooling, can result in a new mid-plane temperature profile. Every radius of the protoplanetary disc is vertically isothermal, but this may only be true in areas with high gas densities and significant thermal conduction. Thermal conduction between the dust and the gas is less effective than gas radiative processes (Baillié & Charnoz 2014).

In a gas disc, the mean opacity of the gas is generally higher than that of the dust at low temperatures, although the Planck opacity of the dust is more significant. However, considering mean opacity separately does not significantly impact the accuracy around the temperature at which the dust sublimates, as the opacity is either dominated by dust or gas (Malygin et al. 2017). The dust opacity at the rim is influenced by both the chemistry and the size distribution. The characteristics of the gas at the inner rim also play a role in shaping the inner rim. Therefore, it is important to calculate the opacity of dust and gas simultaneously in the gas-to-dust transition region (Nagel et al. 2012; Semenov, D. et al. 2003).

Researchers often rely on publicly available opacity tables, such as those compiled by the "OPAL" Project, to study the absorption and scattering of electromagnetic radiation by gases. These tables can simplify the process of determining gas opacities, which can be challenging due to the need to gather data from multiple sources, develop interfaces for reading different types of data, and potentially use computationally intensive methods to calculate line opacities. However, the variation in the chemical equilibrium of the gas can lead to differences in the measured gas temperature between the two opacities in the table(Hirose, Shigenobu et al. 2022).

In the temperature range of 1,000 K to 3,000 K, there is a significant gap in the opacity spectrum between 1-50 micrometres due to the absence of strong absorption bands from any of the species in the gas mixture. This gap becomes more pronounced at low densities but is filled in at high densities due to the pressure-broadening of lines, particularly from alkali atoms. The ionisation of hydrogen at high temperatures reduces its bound-bound source of opacity, leading to a slight decrease in the Planck mean with density but sensitivity to metallicity (Drummond, B. et al. 2018). In our model, the gas Planck mean opacities were calculated under the assumption of a static gaseous disc cloud. However, there is magneto-hydrodynamics wind accretion in the gaseous disc. The minimum values for wind parameters, including mass loss rate, outflow velocity, and dust-to-gas ratio, can be estimated for a given metallicity using Planck models. These wind characteristics tend to lower the overall opacity for any metallicities(Helling et al. 2000).

Two main techniques are used to measure a circumstellar disc's opacity. These methods are used to understand the properties and behavior of the gas and dust within the disc, which can provide insights into the formation and evolution of planetary systems. The Rosseland mean measures the rate of radiative transport (diffusion) in a thick optical gas, while the Planck mean measures the coupling between opacity carrier (dust/gas) and radiation (radiative transfer in an optically thin). The Planck average is three to six orders smaller than the Rosseland means above dust sublimation temperature. This implies Rosseland's mean radiation transport of non-equilibrium radiation is significantly less coupled than Planck's mean (Marleau et al. 2019). The Planck mean is more significantly impacted by metal abundance compared to the Rosseland mean, particularly in the temperature range where metal line cores dominate the Planck mean. The local pressure and temperature dictate the distribution of elements among all the potential chemical species($H_2O, CH_4, and N_2$) in chemical equilibrium. In contrast, the abundance of the individual elements (H_2 and He) fundamentally determines the atmosphere's total chemical composition. These species become more abundant when metallicity rises at the expense of H2 and He (Drummond, B. et al. 2018). There is a significant difference between the Rosseland and Planck mean opacities at high temperatures ($T > 1500K$), where gas species are the main source of opacity. The Planck-mean is significantly influenced by the chosen band and the strength of absorption lines, which vary for different lines and chemical equilibrium constant (Semenov et al. 2003)(Semenov, D. et al. 2003).

There are uncertainties in estimating atomic cross-sections of neutral gases that provide an upper bound uncertainty in opacity (Because of many-body and electron-electron interaction). A lack of Astrophysics research is a major source of uncertainties when calculating opacities (Fontes 2015). Due to the computational complexity of incorporating radiative transport and Astrophysical uncertainty, it is impossible to treat local thermodynamic gas temperatures exactly. The two-temperature Planck opacity ratio exhibits non-monotonic behavior when considering the equilibrium gas temperature as a function of temperature and density. This behavior, described in section 3.3, can result in multiple solutions for the equilibrium gas temperature.

The Planck mean opacity is determined by the local thermodynamic equilibrium of dust and gas at low temperatures, which defines the mass fraction of dust and gas in a circumstellar disc and dictates the radiative transport. There is a significant difference in opacity at the transition between the outermost inner region and the puffed rim due to the sharp temperature differential. In order to smooth this transition, the dust-to-gas ratio was chosen such that "no starlight would be absorbed within a single cell". This is discussed in the study by Schobert, B. N. & Peeters, A. G. (2021).

The gas density in the inner disc of a circumstellar disc can be calculated based on the abundances of different astronomical silicate compositions (derived from Σ_{dust}). The gas surface density at a sublimation radius (0.47 AU) can be estimated using the percentage of each metal (e.g., iron) present in dust grains. However, the gas density cannot be too high, which may affect other disc characteristics (Benisty, M. et al. 2010).

The initial gas surface density profile was taken from Ayliffe & Bate (2009). Still, the gas surface density constant was adjusted through a trial and error to improve the model's accuracy. This was necessary because the data used to calculate the interpolated opacity values was limited in its density range. The refined gas surface density constant was about an order of 10^{-3} magnitude smaller than its original value. When calculating the gas density at the vertical rim using the actual surface density constant, it was found to be $10^{-20} g/cm^3$, much smaller than the expected value Dullemond (1998). The uncertainty of the gas surface density constant is the primary source of error in this calculation. This error was carried through to calculate the optical depth at the inner edge of the rim. The manipulation of the artificial dust and gas density also affects the reliability of the temperature profile. It was found that using a more comprehensive range of density values than those in the table from **?** can improve the accuracy of the equilibrium gas temperature model. However, the specific expression of the surface density constant

did not significantly impact the overall findings of the analysis of the distribution of gas and dust in the disc. In this study, we also examined the properties of rims in discs with low surface densities, assuming that the rims are formed by the evaporation of silicate dust particles of size 1 micron. We found that the surface density of the gas is $10^{-14} g/cm^3$, while the density measured by Benisty, M. et al. (2010) is $10^{-11} g/cm^3$. These differences in density measurements are due to the different treatment of gas and dust opacities, the simplification of radiative hydrodynamics in 1+1D structures, and a lack of knowledge within Astrophysics society. Our results suggest that a low-density region is consistent with the location and characteristics of the rim.

6. Conclusions

This model predicts the temperature profiles and the surface height of the disc and incorporates dust sublimation and radiative transfer with a 1+1D diffusion approximation.

1. The circumstellar disc can be divided into two distinct regions: the gaseous disc and the dusty disc. The gaseous disc extends from the surface of the star, known as the photosphere, to the dust sublimation radius at 0.52 AU. The dusty disc extends from the dust sublimation radius to an outer radius of 100 AU.
2. The model used in this study includes frequency-dependent dust particle opacities and temperature and density-dependent gas opacities to accurately represent the absorption and scattering of radiation in the circumstellar disc. These opacities are important in accurately simulating the interactions of radiation with the gas and dust in the disc.
3. The vertical structure of the circumstellar disc was determined using a 1+1D radiative transport method. However, including thermal conduction, and viscous dissipation improved the accuracy of the temperature profile in the hydrostatic simulation, including in the shadowed region of the disc.
4. The temperature profile in the flared region of the circumstellar disc follows a power law $T \propto r^{-1/2}$, indicating that these regions are primarily influenced by direct irradiation from the central star.
5. The length of the shadowed region within the circumstellar disc, the puffed rim's vertical height, and the puffed rim's position within the disc were observed to vary with metallicity. Higher metallicity leads to a thicker gas disc and lower flux at the inner rim, causing the dust sublimation radius to move closer to the star and the puffed rim to have a smaller vertical height. The length of the shadowed region is also reduced when the metallicity is increased. An increasingly flared disc is observed when the metallicity is $[Me/H] > 0.3$. The temperature profile and vertical structure above the shadowed region were found to have the same characteristics for different metallicities.

Acknowledgements. I would like to thank my supervisor, Dr Tsang, for his support and guidance throughout this project. I am grateful for his consistent help and feedback.

References

Armitage, P. J. 2015, Physical processes in protoplanetary disks
Ayliffe, B. A. & Bate, M. R. 2009, Monthly Notices of the Royal Astronomical Society, 397, 657
Baillié, K. & Charnoz, S. 2014, The Astrophysical Journal, 786, 35
Bell, K. R. 1999, The Astrophysical Journal, 526, 411
Benisty, M., Natta, A., Isella, A., et al. 2010, A&A, 511, A74
Calvet, N., Patino, A., Magris, G. C., & d'Alessio, P. 1991, The Astrophysical Journal, 380, 617
Chiang, E. I. & Goldreich, P. 1997, The Astrophysical Journal, 490, 368
Crida, A. 2009, The Astrophysical Journal, 698, 606
Dong, R. 2015, ApJ, 810, 6
Draine, B. T. & Lee, H. M. 1984, ApJ, 285, 89
Drummond, B., Mayne, N. J., Baraffe, I., et al. 2018, A&A, 612, A105
Dullemond, C. 2012, Chapter 8: Radiative transfer in circumstellar/interstellar media
Dullemond, C. P. 1998, A semi-analytical model of disk evaporation by thermal conduction
Dullemond, C. P., Dominik, C., & Natta, A. 2001, ApJ, 560, 957
Dullemond, C. P. & Natta, A. 2003, A&A, 405, 597
Dullemond, C. P. 2002, A&A, 395, 853
Dullemond, C. P., Henning, Th., Visser, R., et al. 2007, A&A, 473, 457
Dullemond, C. P., van Zadelhoff, G. J., & Natta, A. 2002, A&A, 389, 464
Ferguson, J. W., Alexander, D. R., Allard, F., et al. 2005, The Astrophysical Journal, 623, 585
Flock, M., Fromang, S., Turner, N. J., & Benisty, M. 2016, The Astrophysical Journal, 827, 144
Fontes, C. 2015, Lecture notes in OPACITIES: MEANS UNCERTAINTIES
Gehrig, L., Steindl, T., Vorobyov, E. I., Guadarrama, R., & Zwintz, K. 2022, The influence of metallicity on a combined stellar and disk evolution
Gilman, R. C. 1974, ApJS, 28, 397
Habart, E., Natta, A., & Krügel, E. 2004, A&A, 427, 179
Hahn, J. 2009, The Dynamics of Planetary Systems and Astrophysical Disks (WILEY-VCH)
Helling, C., Winters, J., M, J., & Sedlmayr, E. 2000, åp, 358, 651
Henning, T., Guertler, J., & Dorschner, J. 1983, Ap&SS, 94, 333
Henning, T., Schmitt, W., Klahr, H., & Mucha, R. 1996, in Astronomical Society of the Pacific Conference Series, Vol. 104, IAU Colloq. 150: Physics, Chemistry, and Dynamics of Interplanetary Dust, ed. B. A. S. Gustafson & M. S. Hanner, 513
Hirose, Shigenobu, Hauschildt, Peter, Minoshima, Takashi, Tomida, Kengo, & Sano, Takayoshi. 2022, A&A, 659, A87
Isella, A. & Turner, N. J. 2018, The Astrophysical Journal, 860, 27
Jankovic, M. R., Owen, J. E., Mohanty, S., & Tan, J. C. 2021, Monthly Notices of the Royal Astronomical Society, 504, 280
Jonkheid, B., Faas, F., Zadelhoff, G.-J., & Dishoeck, E. 2004, Astronomy and Astrophysics, 428
Kuiper, R. & Yorke, H. W. 2013, ApJ, 763, 104
Laor, A. & Draine, B. T. 1993, ApJ, 402, 441
Malygin, M. 2016, PhD thesis
Malygin, M. 2016, PhD thesis, Ruprecht-Karls University of Heidelberg, Germany
Malygin, M. G., Klahr, H., Semenov, D., Henning, T., & Dullemond, C. P. 2017, A&A, 605, A30
Malygin, M. G., Kuiper, R., Klahr, H., Dullemond, C. P., & Henning, Th. 2014, A&A, 568, A91
Marleau, G.-D., Mordasini, C., & Kuiper, R. 2019, The Astrophysical Journal, 881, 144
Mathis, J. S., Rumpl, W., & Nordsieck, K. H. 1977, ApJ, 217, 425
Nagel, E., D'Alessio, P., Calvet, N., Espaillat, C., & Trinidad, M. A. 2012, The effect of sublimation temperature dependencies on disk walls around T Tauri stars
Nakatani, R., Hosokawa, T., Yoshida, N., Nomura, H., & Kuiper, R. 2018, ApJ, 857, 57
Natta, A., Testi, L., Calvet, N., et al. 2007, in Protostars and Planets V, ed. B. Reipurth, D. Jewitt, & K. Keil, 767
Pavlyuchenkov, Y. N., Maksimova, L. A., & Akimkin, V. V. 2022, Astronomy Reports, 66, 800
Preibisch, T., Ossenkopf, V., Yorke, H. W., & Henning, T. 1993, A&A, 279, 577
Rodenkirch, P. J., Klahr, H., Fendt, C., & Dullemond, C. P. 2020, A&A, 633, A21
Sabri, T., Gavilan, L., Jäger, C., et al. 2014, ApJ, 780, 180
Schobert, B. N., Peeters, A. G., & Rath, F. 2019, The Astrophysical Journal, 881, 56
Schobert, B. N. & Peeters, A. G. 2021, A&A, 651, A27
Semenov, D., Henning, T., Helling, C., Ilgner, M., & Sedlmayr, E. 2003, Astronomy and Astrophysics, 410
Semenov, D., Henning, Th., Helling, Ch., Ilgner, M., & Sedlmayr, E. 2003, A&A, 410, 611
Setti, G. & Fazio, G. G. 1978, , 4, 89
Shakura, N. I. & Sunyaev, R. A. 1973, A&A, 24, 337
Tsang, D. 2014, The Astrophysical Journal, 782, 112
Vinković, D. 2006, ApJ, 651, 906
Whitehouse, S. C. & Bate, M. R. 2004, Monthly Notices of the Royal Astronomical Society, 353, 1078
Zhang, S., Hu, X., Zhu, Z., & Bae, J. 2021, The Astrophysical Journal, 923, 70